

The GPU-based High-order adaptive OpticS Testbench

Byron Engler^a, Markus Kasper^a, Serban Leveratto^a, Cedric Taissir Heritier^a, Paul Bristow^a,
Christophe Vérinaud^a, Miska Le Louarn^a, Jalo Nousiainen^b, Tapio Helin^b, Markus Bonse^c,
Sascha Quanz^c, Adrian Glauser^c, Julien Bernard^d, Damien Gratadour^e, and Richard Clare^f

^aEuropean Southern Observatory, Karl-Schwarzschild Straße 2, Garching bei Muenchen,
Germany

^bLUT Lappeenranta

^cEidgenössische Technische Hochschule Zürich

^dAustralian National University

^eLaboratoire d'études spatiales et d'instrumentation en astrophysique

^fDepartment of Electrical and Computer Engineering, University of Canterbury, New Zealand

ABSTRACT

The GPU-based High-order adaptive OpticS Testbench (GHOST) at the European Southern Observatory (ESO) is a new 2-stage extreme adaptive optics (XAO) testbench at ESO. The GHOST is designed to investigate and evaluate new control methods (machine learning, predictive control) for XAO which will be required for instruments such as the Planetary Camera and Spectrograph of ESO's Extremely Large Telescope. The first stage corrections are performed in simulation, with the residual wavefront error at each iteration saved. The residual wavefront errors from the first stage are then injected into the GHOST using a spatial light modulator. The second stage correction is made with a Boston Micromachines Corporation 492 actuator deformable mirror and a pyramid wavefront sensor. The flexibility of the bench also opens it up to other applications, one such application is investigating the flip-flop modulation method for the pyramid wavefront sensor.

Keywords: wavefront sensing, adaptive optics, pyramid wavefront sensor, EELT, petaling, segment piston, predictive control, machine learning, extreme adaptive optics, PCS, GHOST

1. INTRODUCTION

The Planetary Camera and Spectrograph (PCS) for the ESO's Extremely Large Telescope (the ELT) will focus on the direct imaging and characterising of nearby exoplanets.¹ The PCS will combine extreme adaptive optics (XAO), coronagraphy (high contrast imaging) and spectroscopy to achieve extremely high contrast between the on-axis starlight and the off-axis light reflected by the planet. The XAO of the PCS will consist of two stages, a slow (1 kHz) loop controlling the first-stage deformable mirror (DM) with approximately 4000 modes, and a high-speed (4 kHz) loop controlling the second-stage DM with on the order of 10000 modes. Predictive control methods, which use past measurements to make predictions of the wavefront at the current time, have an advantage over the traditional integrator controller. A predictive controller will reduce the temporal error and could also reduce the impact of photon noise.² Another potential control method would be to control the point spread function (PSF) contrast directly, instead of directly flattening the wavefront. A promising field of research is using machine learning techniques for both predictive control and PSF contrast control.

The European Southern Observatory (ESO), along with collaborations from external institutes (ETH Zurich, LUT Lappeenranta) has developed the GPU-based High-order adaptive OpticS Testbench (GHOST) as a tool to facilitate the development of predictive control techniques with machine learning in the context of XAO for the PCS. The GHOST is a two-stage XAO system, dimensioned to be similar to the VLT/SPHERE. The first-stage control is performed in simulation, using either a pyramid or Shack-Hartmann wavefront sensor with 40x40 sub-apertures, typically controlling 800-1000 modes at 1 kHz. The residual wavefront error is saved and injected onto

Further author information: (Send correspondence to Byron Engler.)

E-mail: byron.engler@eso.org

Table 1. sLED specifications

Parameter	Value
Model	Thorlabs SLD770S
Centre wavelength	770 nm
Bandwidth	18 nm
Fiber-coupled output power	5.5 mW
Driver	Thorlabs CLD1015

the bench using a spatial light modulator (SLM). The second-stage adaptive optics (AO) control is performed using a pyramid wavefront sensor and a Boston Micromachines Corporation DM, running at an effective speed of 2 kHz to 4 kHz, and controlling 300-400 modes. The Real-time computer (RTC) is built using Commercial off-the-shelf (COTS) server components and two Nvidia enthusiast gaming Graphics processing unit (GPU)s, which will be used for the real-time computation.

2. DESIGN AND IMPLEMENTATION

The GHOST optical design is relatively simple, using on-axis optics and beams splitters and is broken into three separate modules. A schematic of the optical configuration is shown in fig. 1 and a 3D render of the first two modules is shown in fig. 2. The simplicity and modularity of the design allows for straightforward optical alignment, each module can be independently aligned off of the main optical bench. The trade-off with this design is that only 1.5% of the input light makes it to the wavefront sensor (WFS), this is offset by having a powerful light source. The modules are as follows:

- Light source, Spatial Light Modulator (SLM), and DM.
- Coronagraph and PSF imager (‘science’ camera).
- Pyramid WFS, modulation mirror, and pyramid viewing camera. The pyramid WFS has been developed by Arcetri and provided to ESO in the frame of an OPTICON collaboration in 2006. The GHOST is also fully remotely controllable, which proved to be extremely useful during COVID-19 restrictions but also makes the GHOST accessible to anyone with an internet connection.

2.1 Light source

The light source for the GHOST bench is a single-mode fibre-coupled super-luminous light-emitting diode (sLED), sourced from ThorLabs (model number: SLD770S). The sLED has a nominal wavelength of 770 nm with a 18 nm bandwidth, and an output power of 5.5 mW. The sLED is driven with a ThorLabs CLD1015 compact laser diode driver. The CLD1015 controls the current through the LED and the temperature of the diode. The CLD1015 also allows remote control of the light source via a USB connection to a computer.

2.2 Spatial light modulator

The key specification for the SLM selected for the GHOST is the maximum frame rate. The selected SLM, Meadowlark HSP1920-600-1300-HSP8, has a maximum refresh rate of 422.4 Hz. The key specifications for the SLM are listed in table 2. The SLM is provided with a lookup table (LUT), which maps the commanded value (0-255) to phase, for 1550 nm. The provided LUT mapped 0 – 255 to 0 – 2π radians of phase shift. Initially, we simply scaled the LUT to the wavelength of our light source. Using the calibration tools provided by Meadowlark, a custom LUT was measured with the SLM in the GHOST, with a range of 0 – 2π and 0 – 4π . The 0 – 2π LUT gives a smaller phase step size, while the 0 – 4π gives a larger maximum phase shift.

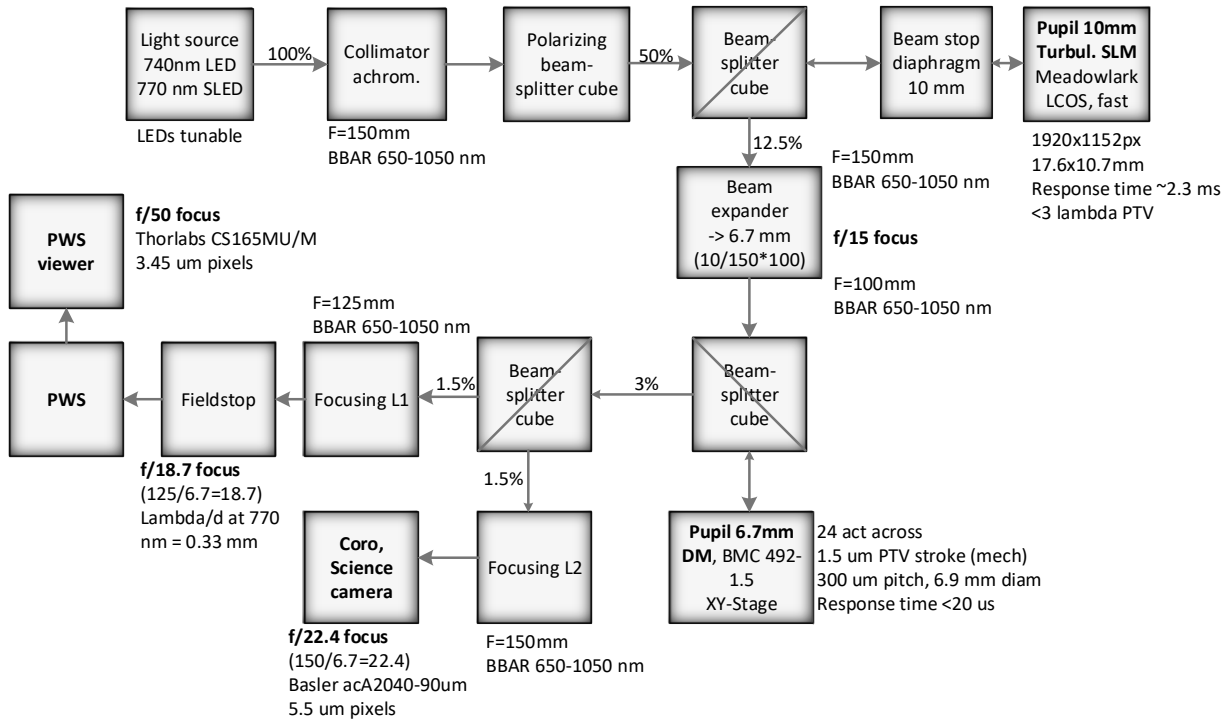


Figure 1. A schematic of the GHOST optics. The light source throughput, beam size and focal ratio are noted at key locations.

Table 2. SLM specifications

Parameter	Value
Model	Meadowlark HSP1920-600-1300-HSP8
Maximum frame rate	422.4 Hz, optical settling time 2.3ms
Resolution	1920 x 1152 pixels
Pixel size	9.2 μ m square
Fill factor	95.7%
Zero-order diffraction efficiency	88%
Control	8-bit, 256 grayscale values
Stroke	4π at 770 nm

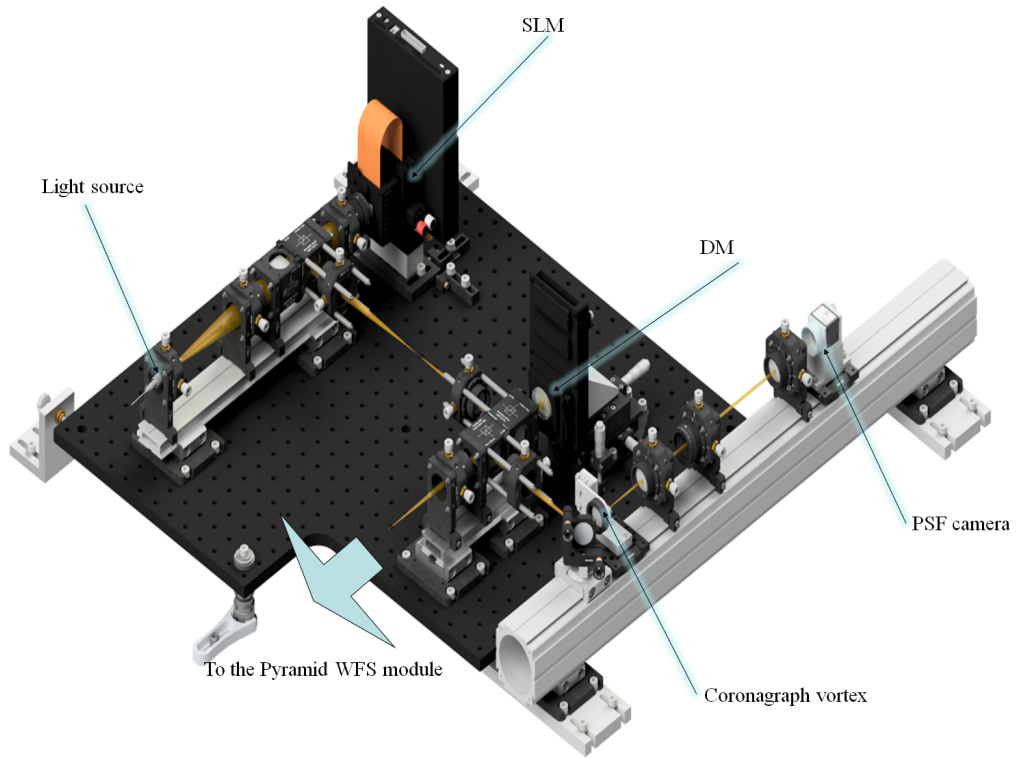


Figure 2. A 3D render of the main optical components of the GHOST bench, showing the light path through the system. The pyramid module is recycled from the High Order Testbench.

Table 3. DM specifications

Parameter	Value
Model	Boston Micromachines Corporation DM 492-C
Actuator grid	24 x 24
Actuator pitch	300 μm
Active aperture size	6.9 mm
Available actuators	492
Stroke	1500 nm mechanical deflection

2.3 Deformable mirror

The deformable mirror is a Boston Micromachines Corporation DM 492-C, which is on loan to ESO from ETH Zurich for the duration of the project. The key parameters of the DM are listed in table 3. The stroke of the DM is not suitable for correction open loop atmospheric turbulence, however, for the application in the GHOST it is ideal as it effectively operates as a second stage DM. The DM driver electronics connects to the RTC via a fibre optic cable connection to a PCIe card provided by Boston Micromachines Corporation.

2.4 Coronagraph and imaging camera

The imaging camera for the GHOST is a Basler ACA2040-90um, the specifications are listed in table 4. The camera arm consists of a vortex coronagraph and the associated relay optics. The camera can be placed in either the focal plane (to image the PSF of the system) or the pupil plane (to adjust the Lyot stop of the coronagraph). The vortex phase plate of the coronagraph is on a motorised XY stage and can be moved in or out of the optical

Parameter	Value
Model	Basler ACA2040-90um
Resolution	2048 x 2048 pixels
Pixel size	5.5 μm square
PSF size ($\frac{\lambda}{D}$)	4 pixels
Vortex mask	Thorlabs WPV10-780

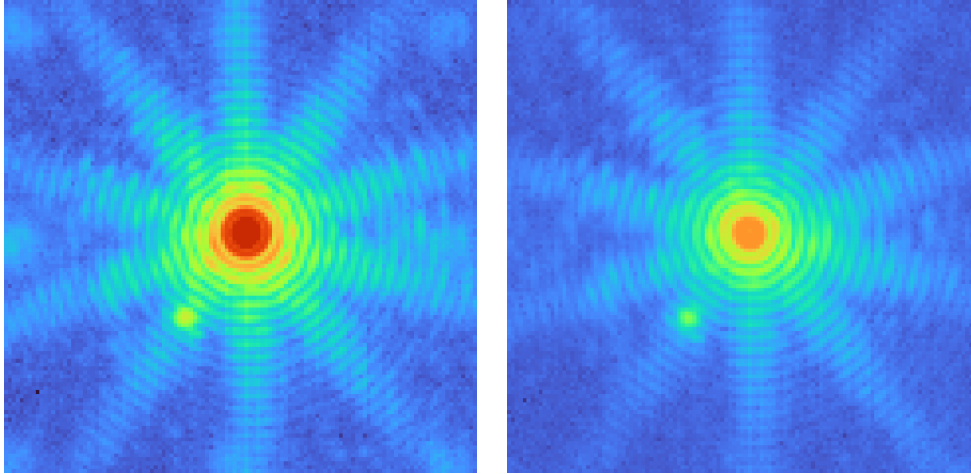


Figure 3. The PSF of the GHOST with the vortex coronagraph moved out of the optical path (left) and in the optical path (right). The speckle in the lower left of the images is due to a reflection (ghost) in the optics.

path as required. Figure 3 shows the PSF of the GHOST, with no turbulence (near-diffraction limited), with and without the coronagraph in place. There is a notable reduction in flux when the coronagraph vortex is in the optical path, however, the reduction is only 2-3 times which is significantly less than desired. Upon investigation, the vortex phase plate was found to have a defect where it has two sweet spots instead of one. We are working with the manufacturer to resolve the issue.

2.5 Pyramid wavefront sensor

The pyramid WFS module has been developed by Arcetri and provided to ESO in the frame of an OPTICON collaboration in 2006, for use on the High Order Testbench (HOT). This module has been recycled, with an upgraded camera. The specifications of the WFS camera are listed in table 5. The modulation tip/tilt mirror

Parameter	Value
Model	Baumer VLXT-06M.I
Resolution	800 x 620 pixels
Pixel size	9.9 μm square
Maximum frame rate (full frame)	1578 fps
PWFS pupil diameter	36 pixels

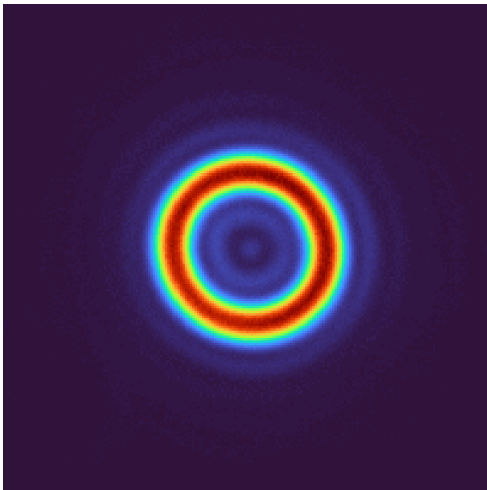


Figure 4. The circularised modulation path, with a radius of $\frac{3\lambda}{D}$ and a modulation frequency of 400 Hz, as seen by the pyramid viewing camera.

Table 6. Pyramid modulation mirror

Parameter	Value
Model	Physik Instrumente SL325
Controller	E-518
Mechanical Resonant Frequency	1 kHz loaded (2 kHz unloaded)

of the pyramid WFS is produced by Physik Instrumente, and the key specifications are listed in table 6. The mirror is actuated by 3 actuators, each with a separation angle of 120° . In order to accurately produce the commanded modulation pattern, the gain and phase delay of each actuator is first measured using the position sensors built into the actuators. Figure 5 shows the gain and phase response of the modulation mirror for a range of modulation frequencies. Knowing the gain and phase delay for each actuator, a suitable command can be found such that the modulation path is circular. However, due to the optical configuration, the gain on one axis is less than on the other, without an optical calibration the modulation path would not be circular. For the purpose of optically calibrating the modulation path, a pyramid viewing camera was added to the pyramid WFS module. A pellicle beamsplitter is inserted just in before the pyramid which diverts light to a pyramid viewing camera, effectively measuring the focal plane in which the pyramid is placed. This allows the modulation mirror to be calibrated such that the modulation radius is known in $\frac{\lambda}{D}$, as well as the optical gain for each of the actuators. Figure 4 shows the modulation path as seen by the pyramid viewing camera, with a corrected circular modulation.

2.6 Real-time computer

The real-time computer consists of COTS server components, with two Nvidia gaming GPUs. The major components of the computer are listed in table 7. The GHOST will use the COSMIC RTC platform, making use of the GPUs in the computer. COSMIC is a hard real-time adaptive optics controller, implemented on Nvidia GPUs.³ Partnering with the Australian National University and LESIA, the COSMIC platform has been installed on the GHOST. Figure 6 shows the COSMIC pipeline implemented for the GHOST.

3. ADAPTIVE OPTICS CALIBRATION

For the purpose of commissioning and adaptive optics calibration, a graphical user interface (GUI) has been developed using Python. The NumPy library, compiled with the Intel MKL BLAS and LAPACK, is used for

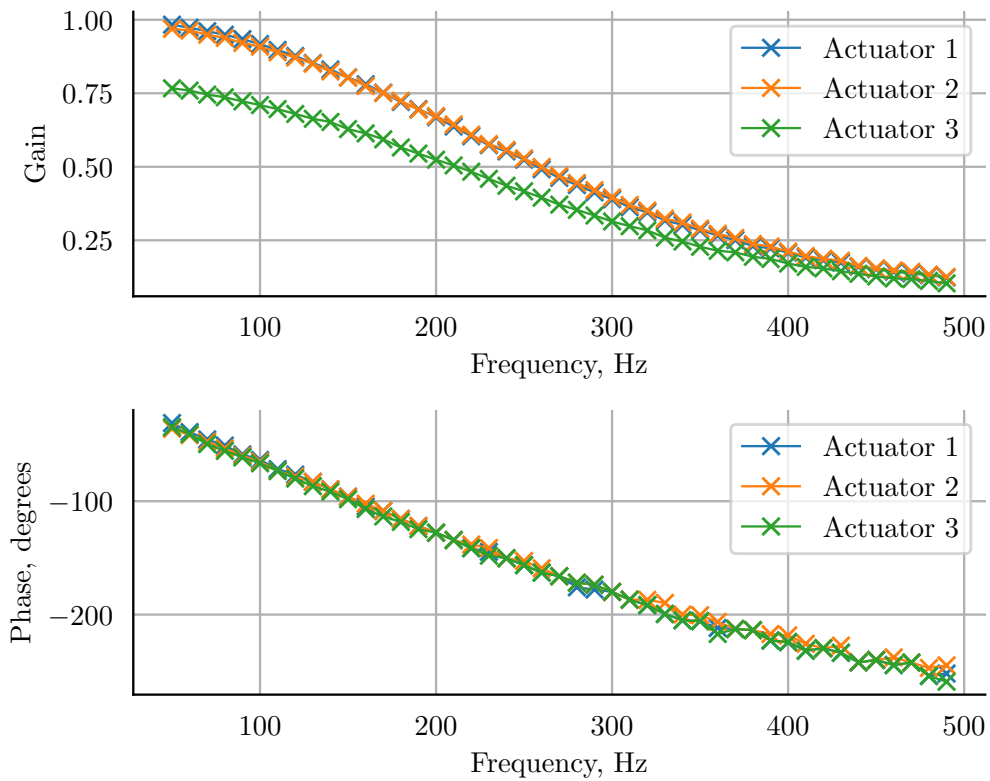


Figure 5. The closed-loop gain and phase response of each actuator whilst modulation at a range of frequencies. The measurements are made using the strain gauges built into each actuator of the modulation mirror.

Table 7. Real-time computer

Parameter	Value
CPU	2x Intel(R) Xeon(R) Gold 6258R (112 threads total)
RAM	192 GB DDR4 (12 x 16GB)
GPU	2x Nvidia RTX Titan with NVlink bridge

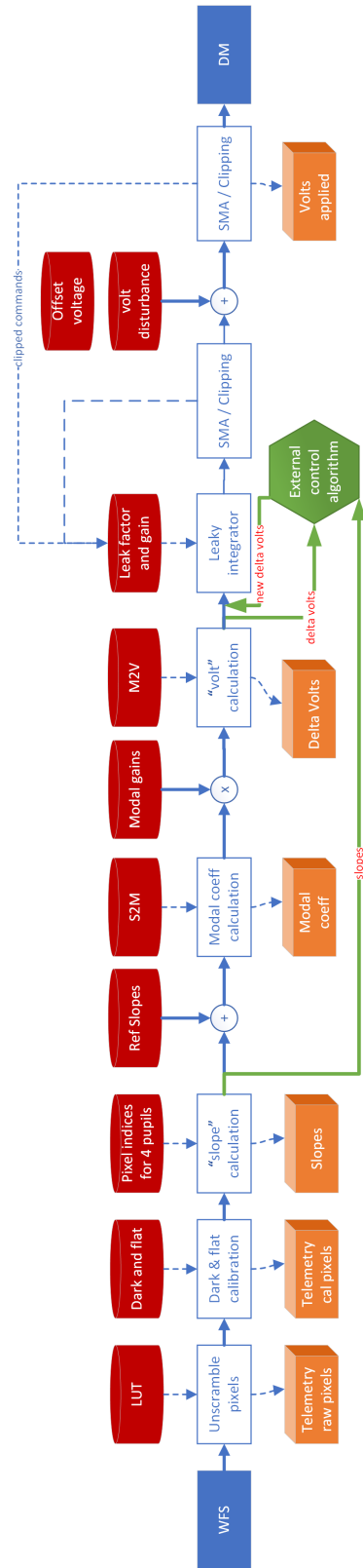


Figure 6. The real-time pipeline implemented using the COSMIC RTC.

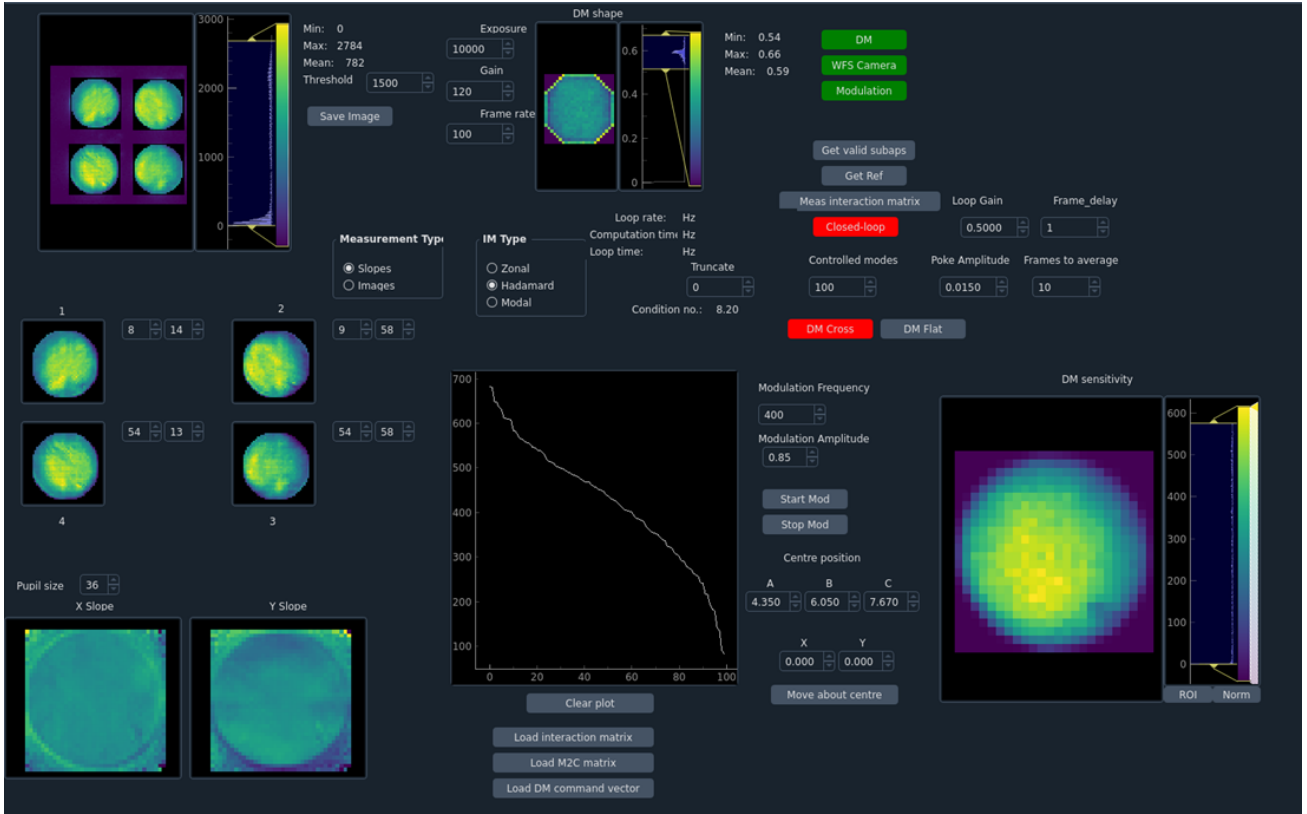


Figure 7. The graphical user interface developed in Python using PyQt5 and PyQtGraph, for the alignment and adaptive optics calibration, and closed-loop control. The plot at the top left is the latest image from the wavefront sensor. The four pupils are masked, and the cut-outs are shown immediately below. Below the pupil cutouts are the x and y slopes. The plot in the centre shows the eigenvalues of the control matrix. The figure at the top right shows the current DM command. The plot at the bottom right shows the sensitivity of the DM actuators in the WFS space.

all of the computation, PyQt5 is used for the GUI and PyQtGraph is used for the real-time figures. The GUI is shown in fig. 7, after completion of the AO calibration. The GUI is also capable of closed-loop AO control.

The calibration of the AO system is achieved by actuating the DM with Hadamard patterns, and the resulting WFS signals are decoded and inserted into a zonal interaction matrix.⁴ Mathematically, the calibration procedure is for a system with n actuators and m slope measurements, expressed as

$$C = DV + N, \quad (1)$$

where C is an $m \times n$ matrix containing WFS slope measurements, V is an $n \times n$ matrix containing the actuation patterns, and D is an $m \times n$ and is the interaction matrix relating slopes to actuation patterns. An estimation of the interaction matrix, \hat{D} , is then

$$\hat{D} = CV^{-1}. \quad (2)$$

A Hadamard matrix is an orthogonal square matrix containing only 1's and -1's. The inverse of a Hadamard matrix of size n , H_n is then

$$H_n^{-1} = H_n^T. \quad (3)$$

If we actuate the DM with Hadamard patterns,

$$V = v_m H_n, \quad (4)$$

where v_m is a scalar, then the interaction matrix can be estimated as

$$\hat{D} = CV^T. \quad (5)$$

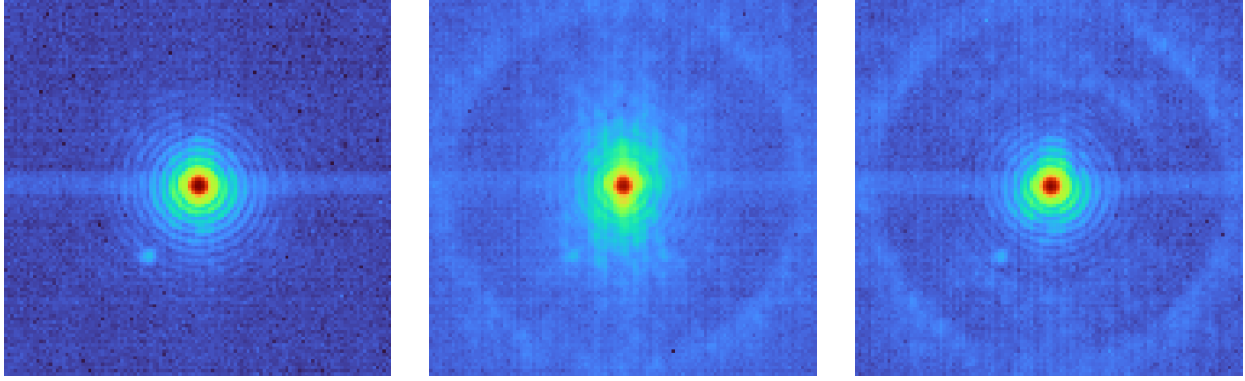


Figure 8. The long exposure point spread functions measured with the focal plane imager. From left to right: The diffraction PSF of the system, the PSF with AO residuals from the simulated first stage where the control radius of the first stage is visible (900 modes controlled), and the PSF with the 2nd stage loop closed where the control radius of the second stage is clearly visible, with 350 controlled modes. The speckle in the upper left quadrant is a reflection (ghost) in the system.

In the case of the GHOST, the nearest Hadamard matrix has a size of $n = 512$. In this case, the DM commands are truncated to the number of actuators (492). For modal control, the modal basis is then projected onto the zonal interaction matrix, giving a modal interaction matrix. The pseudo-inverse of the modal interaction matrix is then used as the control matrix.

4. CURRENT STATUS AND APPLICATIONS OF GHOST

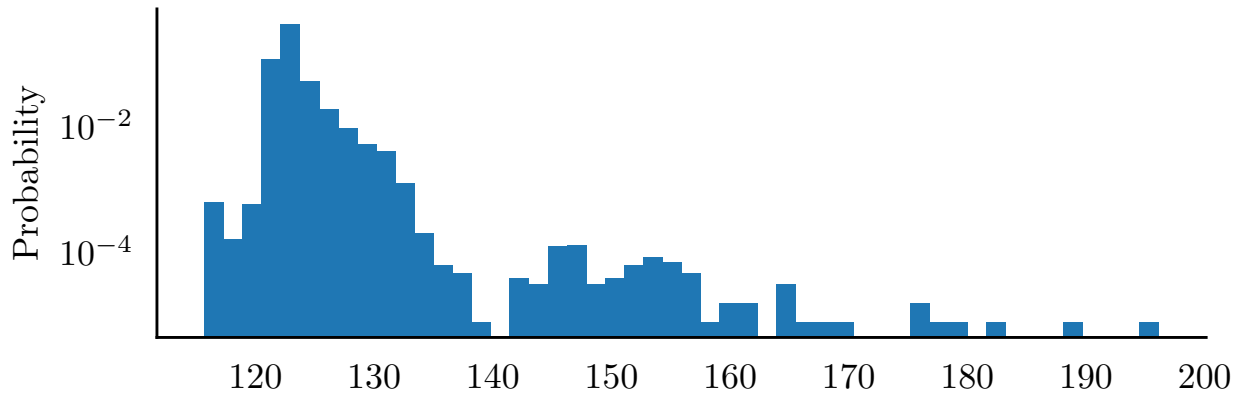
The GHOST is fully operational, fig. 8 shows the long exposure PSFs measured with the PSF camera for the diffraction-limited case (no turbulence), the open-loop (1st stage closed-loop residuals) case, and the closed-loop (2nd stage closed) case. The computation time for the closed-loop calculations (time from receiving the image to sending the DM commands) for both the COSMIC GPU RTC and Python-based commissioning GUI are shown in fig. 9 whilst controlling 300 modes. The GPU-based COSMIC RTC achieves an average latency of 123 μ s whilst the CPU-based Python GUI archives an average latency of 964 μ s. No special effort has been made to optimise the Python GUI and as such there are large spikes in latency. The GHOST is already in use, with three papers presented at the SPIE Astronomical Telescopes + Instrumentation 2022 conference making use of the GHOST:

- Advances in model-based reinforcement learning for AO control – Jalo Nousiainen - Paper 12185-302
- Detection of discontinuous phase steps with a pyramid wavefront sensor – Deborah Malone - Paper 12185-200
- Experimental verification of a Neural Network and PCA approach for NCPA mitigation - Alessandro Terreri - Paper 12185-314

Whilst the GHOST is intended to explore new control methods for XAO, it is fully equipped for other experiments which require a pyramid wavefront sensor, a high order DM, and a method to inject arbitrary phase screens. One such application is exploring flip-flop modulation,⁵ where the pyramid wavefront sensor is operated in both a modulated and unmodulated state. A key question posed by the flip-flop modulation method is whether the modulator could be stopped and started rapidly. Figure 10 shows the commanded and measured modulation path at 100Hz and 400Hz. In both cases, the modulator can start and stop within a single modulation cycle.

Using the parameters in table 8, the flip-flop modulation is compared to a normal circular modulation pattern. Figure 11 compares the root mean square of the residual wavefront error and the resulting long exposure PSFs are shown in fig. 12. For the normal modulation case, a continuous modal basis⁶ is used. To create the continuous basis used, the Karhunen-Loève (KL) modes are defined on a circular pupil geometry, without spiders. The flip-flop modulation uses petal eigenmodes for the unmodulated pyramid, and KL modes defined with the pupil geometry (with spiders) and forced to be orthogonal to the petal eigenmodes are used for the modulated pyramid.

COSMIC - GPU



Python - CPU

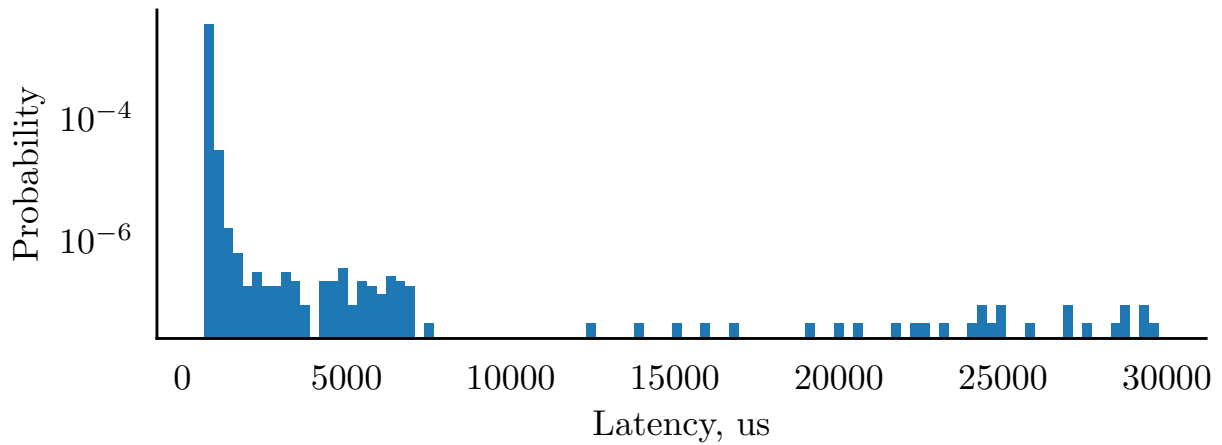


Figure 9. The latency and jitter from WFS image received to DM commands sent for the COSMIC RTC and the Python AO CPU implementation.

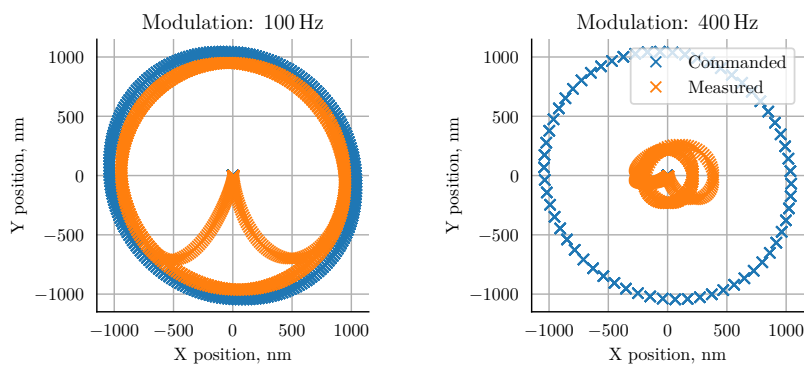


Figure 10. The commanded and measured modulation path at 100Hz (left) and 400Hz (right). The commanded paths have been corrected to produce a circle at the tip of the pyramid. The actuators of the modulation mirror have a frequency-dependent gain and phase shift, which need to be considered for each modulation frequency. The modulator is clearly able to start and stop within the one frame required for flip-flop modulation at both 100Hz and 400Hz.

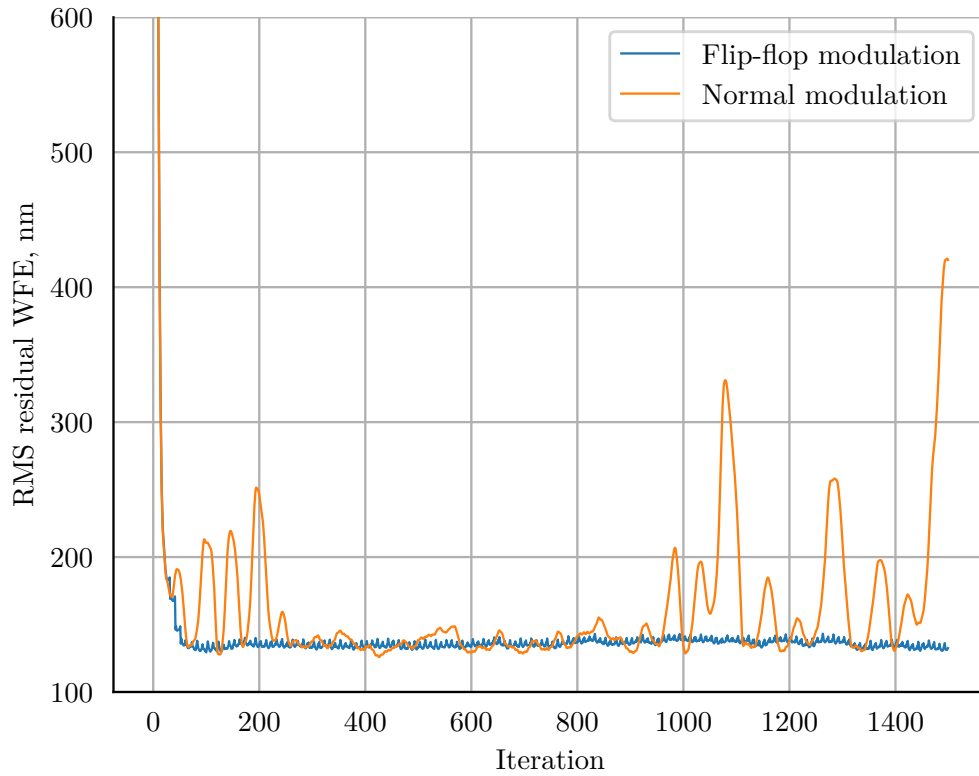


Figure 11. A simulation comparing the flip-flop modulation method (orange) with ‘normal’ modulation (blue). The root mean square of the residual wavefront error is plotted at each iteration. The atmosphere has an r_0 of 15 cm and the wavefront sensor is in R-band.

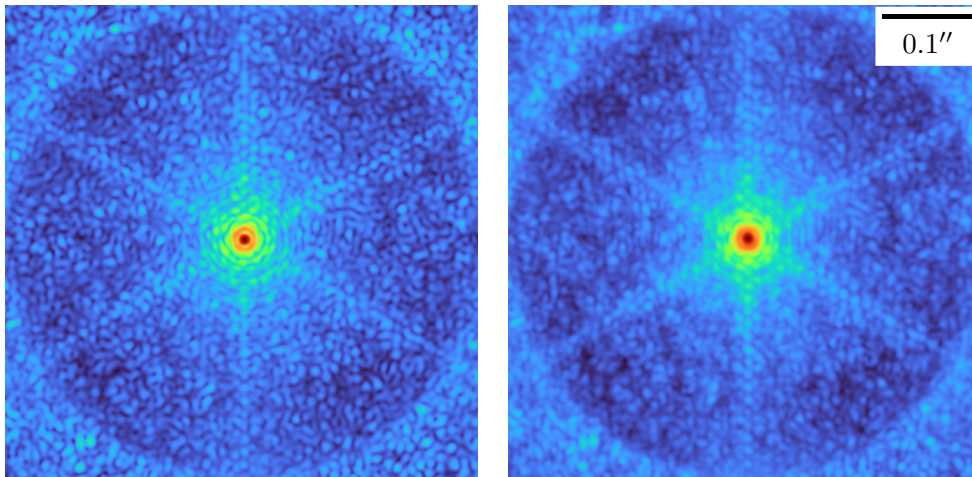


Figure 12. The simulated long exposure point spread function in R-band, with the WFS operating in R-band, with flip-flop modulation (left) and normal modulation (right).

Table 8. Simulation parameters used for flip-flop modulation.

Parameter	Value
Telescope Diameter (D)	40 m
Secondary Obstruction	28%
Fried Parameter (r_0)	15 cm
Outer Scale (L_0)	30 m
Atmosphere	single layer
Frame Rate (F_s)	1 kHz
Delay	2 Frames
Controller Type	Integrator
PSF (λ_p) Wavelength	640 nm (R-band)
WFS (λ_W) Wavelength	640 nm (R-band)
WFS Order	116×96 Subapertures
Modulation Width	$4\lambda_W/D, 0\lambda_W/D$
Time Steps	1500
Number of Spider Arms	6
Spider Arm Width	51 cm
Flux	10000 photons/subaperture/frame
Number of Actuators	5190
Number of Modes	3500

5. CONCLUSION

This paper presents the design and implementation of the GHOST which enables the development of predictive control in the context of XAO for PCS. The GHOST is a 2-stage XAO system, where the first stage is simulated, with first stage residual turbulence injected to the bench with a high-speed SLM. The GHOST is fully operational and being actively used, the first stage (simulated and injected onto the bench with the SLM) controls 800-1000 modes whilst the second stage controls 300-400 modes, at a loop rate of up to 400 Hz (emulating a loop rate of up to 4 kHz). Whilst GHOST has been designed to develop predictive control algorithms, it also provides a general purpose AO testbed, which is remotely accessible, controllable via Python interfaces and easy to implement new control ideas on.

6. ACKNOWLEDGEMENTS

The authors would like to thank ESO’s technology development programme, which has helped fund the development of the GHOST.

REFERENCES

- [1] Kasper, M., Cerpa Urra, N., Pathak, P., Bonse, M., Nousiainen, J., Engler, B., Heritier, C. T., Kammerer, J., Leveratto, S., Rajani, C., Bristow, P., Le Louarn, M., Madec, P. Y., Ströbele, S., Verinaud, C., Glauser, A., Quanz, S. P., Helin, T., Keller, C., Snik, F., Boccaletti, A., Chauvin, G., Mouillet, D., Kulcsár, C., and Raynaud, H. F., “PCS — A Roadmap for Exoearth Imaging with the ELT,” *The Messenger* **182**, 38–43 (Mar. 2021).
- [2] Males, J. R. and Guyon, O., “Ground-based adaptive optics coronagraphic performance under closed-loop predictive control,” *Journal of Astronomical Telescopes, Instruments, and Systems* **4**(1), 1 – 21 (2018).
- [3] Ferreira, F., Sevin, A., Bernard, J., Guyon, O., Bertrou-Cantou, A., Raffard, J., Vidal, F., Gendron, E., and Gratadour, D., “Hard real-time core software of the AO RTC COSMIC platform: architecture and performance,” in [*Adaptive Optics Systems VII*], Schreiber, L., Schmidt, D., and Vernet, E., eds., **11448**, 239 – 254, International Society for Optics and Photonics, SPIE (2020).

- [4] Kasper, M., Fedrigo, E., Looze, D. P., Bonnet, H., Ivanescu, L., and Oberti, S., “Fast calibration of high-order adaptive optics systems,” *J. Opt. Soc. Am. A* **21**, 1004–1008 (Jun 2004).
- [5] Engler, B., Louarn, M. L., Vérinaud, C., Weddell, S., and Clare, R. M., “Flip-flop modulation method used with a pyramid wavefront sensor to correct piston segmentation on ELTs,” *Journal of Astronomical Telescopes, Instruments, and Systems* **8**(2), 1 – 16 (2022).
- [6] Bertrou-Cantou, A., Gendron, E., Rousset, G., Ferreira, F., Sevin, A., Vidal, F., Clénet, Y., Buey, T., and Karkar, S., “Petalometry for the ELT: dealing with the wavefront discontinuities induced by the telescope spider,” in [*Adaptive Optics Systems VII*], Schreiber, L., Schmidt, D., and Vernet, E., eds., **11448**, 213 – 224, International Society for Optics and Photonics, SPIE (2020).